ECCOMAS Congress 2016
VII European Congress on Computational Methods in Applied Sciences and Engineering
M. Papadrakakis, V. Papadopoulos, G. Stefanou, V. Plevris (eds.)
Crete Island, Greece, 5–10 June 2016

A LAGRANGIAN PFEM APPROACH TO THE NUMERICAL SIMULATION OF 3D LARGE SCALE LANDSLIDES IMPINGING IN WATER RESERVOIRS

M. Cremonesi[1], **F. Ferri**[1], **and U. Perego**[1]

[1]Department of Civil and Environmental Engineering
Politecnico di Milano
Piazza Leonardo da Vinci, 32, 20133, Milano, Italy
e-mail: {massimiliaano.cremonesi,francesco.ferri,umberto.perego}@polimi.it

Keywords: PFEM, landslides, water reservoir, Lagrangian approach.

Abstract. *Landslides are exceptional natural hazards that can generate extensive damage to structures and infrastructures causing a large number of casualties. A particularly critical condition occurs when the landslide impinges in water reservoirs generating high waves. This work proposes a numerical tool to simulate the macroscopic behavior of a propagating landslide. The Particle Finite Element Method (PFEM) is here used and adapted to the specific case of landslide runout. The Lagrangian Navier-Stokes equations of incompressible fluids are used to describe the macroscopic landslide behavior. A rigid-visco-plastic law with a pressure dependent threshold, typical of a non-Newtonian, Bingham-like fluid, is used to characterize the constitutive behavior of the flowing material. Special attention is devoted to the definition of ad-hoc pressure-dependent slip boundary conditions at the interface between the flowing mass and the basal surface to better represent the real landslide-slope interaction. The proposed approach has been validated against numerical benchmarks and small scale experimental tests, showing a good agreement with the physical measurements. Real case scenarios have also been considered. 3D geometries of critical sites, where landslides have occurred, have been reconstructed allowing for the simulation of large scale real landslide runouts. Results are compared with post-event images and measurements, showing the accuracy and the capability of the method.*

1 INTRODUCTION

Catastrophic landslides impinging into water reservoirs may generate impulsive waves whose propagation can cause considerable damages. Instability of a slope can be triggered by natural events (erosion, earthquakes, intense rainfalls) or by human activities (deforestation, construction). Once initiated, a landslide can run along a slope with different velocities and cover long distances, depending also on the slope morphology. The prediction of landslides velocity, runout distance and traveling path is useful for preventing and mitigating the consequences of these events.Consequently, the interest for numerical tools capable to simulate landslides with potentially long run-out distance, including their interaction with water basins, is continuously growing.

Recent developments in the simulation techniques for coupled problems have led to efficient analysis procedures allowing for the accurate reproduction of landslide-reservoir interactions (see for example [1, 2]). The numerical analysis of these events requires capabilities for tracking interfaces and free surfaces undergoing large displacements, and accounting for the mixing of different constituents, for complex constitutive behaviors and for multi-physics processes. In this work, a recently developed Lagrangian finite element approach [3, 4, 5], formulated in the spirit of the Particle Finite Element Method (PFEM), is here reconsidered and adapted to the specific case of landslide-reservoir interaction. The PFEM was originally developed [5, 6, 7] for solving problems involving free surfaces fluid flows and fluid-structure interaction. The Lagrangian nature of the approach allows for a natural treatment of free surfaces undergoing large displacements and of fast evolving interfaces, making the method particularly suitable for the simulation of landslide phenomena and of landslide-water interaction problems, which are dominated by fast propagating waves and interfaces. Due to the excessive distortion of the mesh, typical of Lagrangian approaches for fluids, a continuous remeshing, based on a fast 3D Delaunay triangulation, is implemented. A 3D version of the alpha-shape technique [5] is used to define the position and the evolution of the free-surfaces. New slip boundary conditions of Navier type have been formulated to model the interaction between the sliding material and the basal surface. The PFEM formulation has been modified to incorporate these new conditions.

2 GOVERNING EQUATIONS

The running landslide material is assumed to behave as a rigid-viscoplastic fluid. As a consequence, both landslide and water motions are governed by Navier-Stokes equations (here written in an Arbitrary Lagrangian-Eulerian framework [8]):

$$\begin{aligned} \rho\left(\frac{\partial \mathbf{u}}{\partial t} + (\mathbf{c}\cdot\nabla_x)\mathbf{u}\right) &= \nabla_x\cdot\boldsymbol{\sigma} + \rho\mathbf{b} \quad \text{in } \Omega_t\times(0,T) \\ \nabla_x\cdot\mathbf{u} &= 0 \quad \text{in } \Omega_t\times(0,T) \end{aligned} \tag{1}$$

where ∇_x is the gradient spatial operator computed with respect to the current configuration, $\boldsymbol{\sigma}$ is the Cauchy stress tensor, ρ is the density and and $\mathbf{b}$ are the external body forces. The convective velocity $\mathbf{c}$ is defined as:

$$\mathbf{c} = \mathbf{u} - \mathbf{r} \tag{2}$$

$\mathbf{u}$ being the velocity of the fluid and $\mathbf{r}$ the mesh velocity. In general, an additional equation governing the evolution of the mesh $\mathbf{r}$ is necessary. The standard Eulerian description of the equation of motion can be recovered when $\mathbf{r} = 0$ (i.e. $\mathbf{c} = \mathbf{u}$). Conversely, the Lagrangian description is obtained with $\mathbf{r} = \mathbf{u}$ (i.e. $\mathbf{c} = 0$). As a consequence, in the Eulerian approach

the mesh is fixed, while in the Lagrangian one the mesh moves with the velocity of the fluid particles.

Equations (1) need be supplemented with proper initial and boundary conditions. The boundary $\partial\Omega_t$ is partitioned into three non-overlapping subsets $\partial\Omega_t = \Gamma_t^D \cup \Gamma_t^N \cup \Gamma_t^S$. On Γ_t^D and Γ_t^N standard Dirichlet and Neumann boundary conditions are imposed, while on Γ_t^S slip boundary conditions are considered. On Γ_t^D Dirichlet boundary conditions are imposed on velocities and on Γ_t^N Neumann boundary conditions are imposed on surface tractions:

$$\begin{aligned} \mathbf{u}(\mathbf{x},t) &= \bar{\mathbf{u}}(\mathbf{x},t) \qquad \text{on } \Gamma_t^D \\ \boldsymbol{\sigma}(\mathbf{x},t)\cdot\mathbf{n} &= \mathbf{h}(\mathbf{x},t) \qquad \text{on } \Gamma_t^N \end{aligned} \tag{3}$$

where $\bar{\mathbf{u}}(\mathbf{x},t)$ and $\mathbf{h}(\mathbf{x},t)$ are assigned functions and $\mathbf{n}$ is the outward normal to the boundary.

3 CONSTITUTIVE LAW

Both the landslide and the reservoir water are modeled as viscous fluids. The Cauchy stress tensor $\boldsymbol{\sigma} = \boldsymbol{\sigma}(\mathbf{x},t)$ is decomposed into its hydrostatic p and deviatoric $\boldsymbol{\tau}$ components as $\boldsymbol{\sigma} = -p\mathbf{I} + \boldsymbol{\tau}$ where $\mathbf{I}$ the identity tensor. Water is assumed to be a Newtonian isotropic incompressible fluid so that the deviatoric stress $\boldsymbol{\tau}$ can be directly related to the symmetric part of the velocity gradient:

$$\boldsymbol{\tau} = \frac{1}{2}\mu\left(\nabla\mathbf{u} + \nabla\mathbf{u}^T\right) \tag{4}$$

where μ is the dynamic viscosity.

Unlike in standard Navier-Stokes formulations, the landslide material is assumed to obey a regularized elastic-viscoplastic non-Newtonian, Bingham-like constitutive model. When external actions trigger the landslide motion and the yield limit is exceeded, large viscoplastic deformations take place and the running landslide behaves as a viscoplastic Bingham fluid. In the assumed model the deviatoric stress follows again the relation (4), but the dynamic viscosity μ is replaced by the apparent viscosity $\widetilde{\mu}$ defined as:

$$\widetilde{\mu} = \mu + \frac{p\,\tan(\varphi)}{|\dot{\gamma}|}\left(1 - e^{-n|\dot{\gamma}|}\right) \tag{5}$$

where φ is the friction angle and $|\dot{\gamma}|$ represents a norm of the symmetric part of the velocity gradient. The exponential term in (5) has only a regularization purpose [2, 9], and does not have a constitutive interpretation. The constitutive law expressed by equation (5) can be interpreted as a viscoplastic behavior with a Drucker-Prager type yield criterion. A detailed description of the derivation of this model can be found in [10].

4 SLIP CONDITIONS

Along the boundary Γ_t^S, Navier type slip boundary conditions with a pressure dependent threshold are enforced:

$$\mathbf{u}_{slip} = -\beta\frac{\mathbf{t}}{\|\mathbf{t}\|}\langle\|\mathbf{t}\| - p\tan\varphi_{basal}\rangle \tag{6}$$

where $\mathbf{u}_{slip}$ is the velocity at the interface and $\mathbf{t}$ the traction force defined as (see also Figure 1 for a graphical representation):

$$\mathbf{t} = (\mathbf{I} - \mathbf{n}\otimes\mathbf{n})\,(\boldsymbol{\sigma}\mathbf{n}) \tag{7}$$

being $\beta = h_{slip}/\mu$ a parameter, having the dimension of a length over a viscosity, characterizing the basal interface, h_{slip} is the slip length for an ideal Couette flow with no threshold ($\varphi_{basal} = 0$) and φ_{basal} is the friction angle of the basal interface.

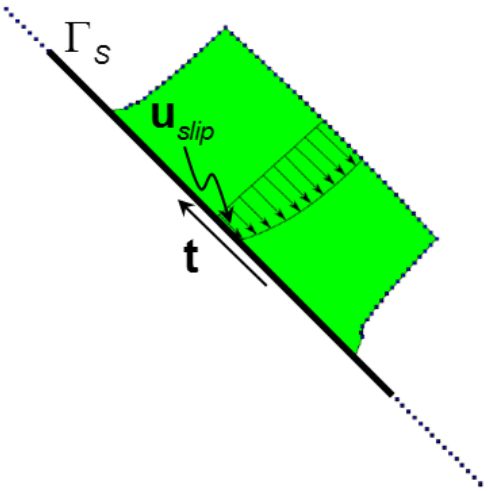

Figure 1: Slip velocity profile and basal tangential traction.

5 DISCRETIZATION AND NUMERICAL TECHNIQUE

Slip boundary conditions are difficult to enforce in a fully Lagrangian framework, in which nodes on the basal surface move according to their own velocity, but at the same time, in view of the PFEM remeshing strategy, have to define the position of the boundary. To overcome this difficulty, all nodes in the mesh are treated as Lagrangian (i.e. $\mathbf{c} = \mathbf{0}$ in eq. 1) except those on Γ^S (where slip conditions are imposed), which are treated as Eulerian (i.e. $\mathbf{c} = \mathbf{u}$) and therefore remain fixed in their initial position. This special treatment gives rise to a mixed Lagrangian-Eulerian formulation, where some nodes are Lagrangian and others are Eulerian.

A classical Galerkin Finite Element procedure is used to discretize the problem in space with linear interpolation functions for both pressure and velocity. The following semidiscretized form is obtained:

$$\mathbf{M}\dot{\mathbf{U}} + (\mathbf{K} + \mathbf{K}_{slip} + \mathbf{K}_c)\mathbf{U} + \mathbf{D}^T\mathbf{P} = \mathbf{B} \tag{8}$$

$$\mathbf{D}\mathbf{U} = \mathbf{0} \tag{9}$$

where $\mathbf{U}$ and $\mathbf{P}$ contain the nodal values of velocity and pressure respectively, $\mathbf{M}$ is the mass matrix, $\mathbf{K}$ is the matrix of viscoplastic coefficients, $\mathbf{D}$ is the discretization of the divergence operator, $\mathbf{B}$ is the vector of body forces and boundary tractions (see [3] for the definition of these matrices). $\mathbf{K}_c$ represents the discretization of the convective term on the slip boundary and $\mathbf{K}_{slip}$ is the discretization of the integral slip term. The contribution to matrices $\mathbf{K}_c$ and $\mathbf{K}_{slip}$ by all elements with no nodes on Γ^S is zero. A detailed description of these matrices can be found [10].

Introducing now a backward Euler integration scheme for the time integration, the final fully

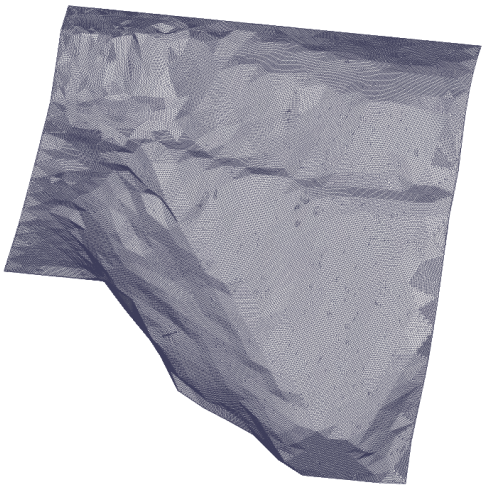

Figure 2: Cougar Hill. Finite element mesh used in the simulation.

discretized nonlinear problem writes:

$$\left(\frac{\mathbf{M}}{\Delta t}+\mathbf{K}+\mathbf{K}_{slip}+\mathbf{K}_c\right)\mathbf{U}^{n+1}+\mathbf{D}^T\mathbf{P}^{n+1}=\mathbf{B}^{n+1}+\frac{\mathbf{M}}{\Delta t}\mathbf{U}^n \tag{10}$$

$$\mathbf{D}\mathbf{U}^{n+1}=\mathbf{0} \tag{11}$$

The Lagrangian PFEM is here used to solve the differential problem (10-11). In the spirit of the Particle Finite Element Method, to avoid excessive mesh distortion due to the Lagrangian nature of the equations, the domain is frequently remeshed. An index of the element distortion is used to check whether the mesh should be regenerated or not. When a new mesh has to be created, a Delaunay tessellation technique is used to redefine the element connectivities starting from the current nodal positions. Moreover, an "alpha shape" technique is introduced to identify the free-surfaces and the interacting surfaces between water and landslide. Details on the numerical procedure can be found in [2, 3, 4, 5].

6 NUMERICAL EXAMPLES

6.1 Cougar Hill Landslide

The real event considered in this test case took place on Rocky Mountain in west Canada in 1992 [11]. Approximately 200 000 m^3 of debris started to flow from a 100 m high dump; the material stopped to flow after about 700 meters. The dump slope angle was estimated to be $37°$-$38°$. According to [11], the debris material was mainly sandy gravel and the foundation was composed by sand and gravel colluvium. The material parameters can be found in Table 1. Density and friction angles are provided in [11] while viscosity and slip length are estimated through back analysis.

Numerical results on the same example as well as some interesting discussions can be found in [12, 1, 13]. The 3D CAD model of the terrain (kindly provided by prof. M. Pastor) is plotted in figure 2. For the numerical analysis, a finite element mesh of 106046 nodes has been used with a fixed time step of $5 \cdot 10^{-3}$ seconds. The real time simulated in the analysis is 100 s.

Results are shown in Figure 3, where contour plots of the velocity at different time instants are plotted, and are in good agreement with results of other simulations available in the literature. Moreover, in Figure 4 the final deposit obtained with the present approach is compared with the result of the post-failure geotechnical investigations proposed in [11].

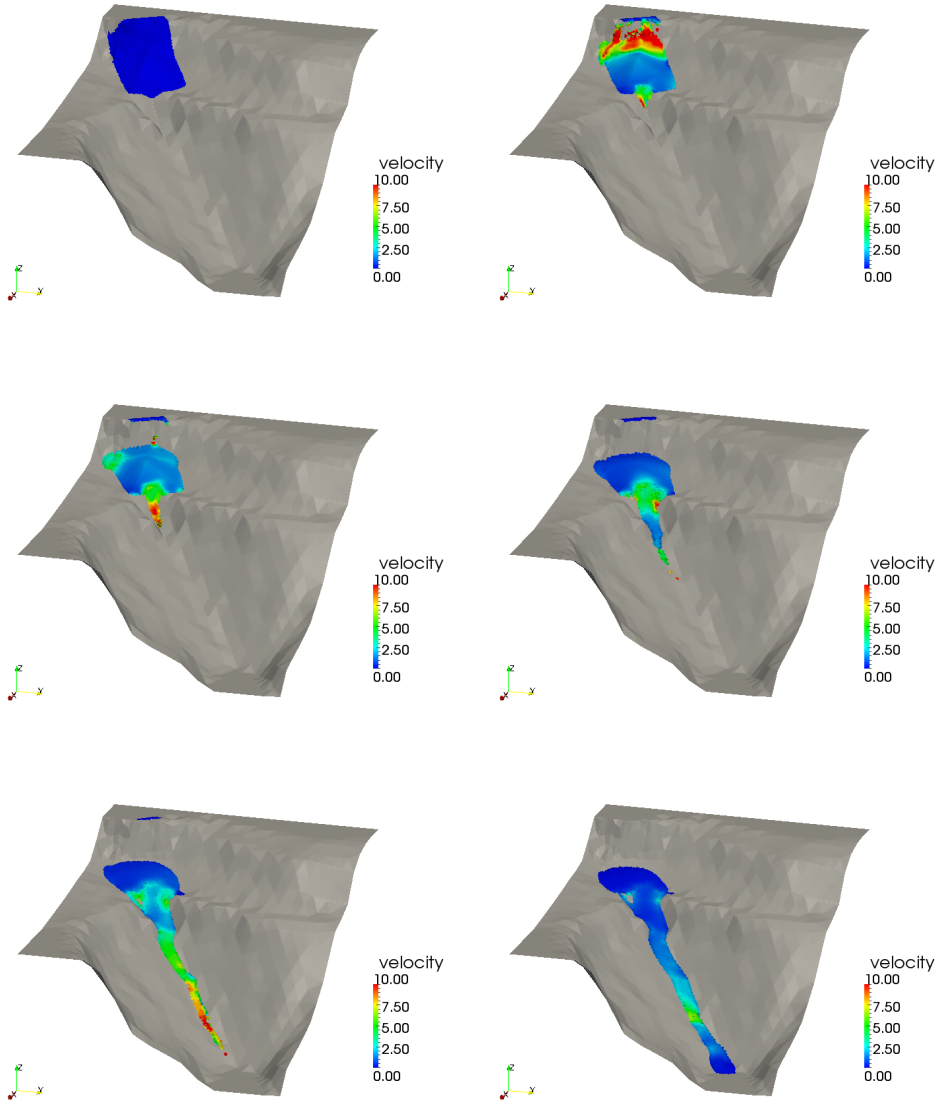

Figure 3: Cougar Hill. Velocity contour plots at t=0, 5, 20, 30, 70, 110 seconds.

ρ	$1.9\ 10^3\ Kg/m^3$
ϕ	$32°$
ϕ_{basal}	$28°$
μ_0	$0.01\ Pa\ s$
h_{slip}	$4\ m$

Table 1: Cougar Hill. Material parameters.

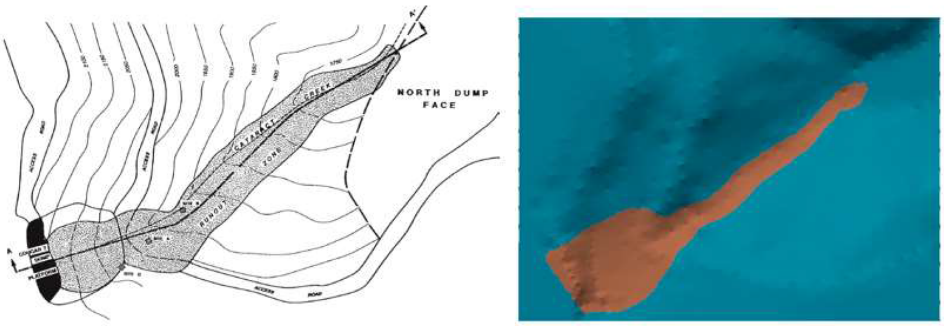

Figure 4: Cougar Hill. Comparison of the final deposit.

7 Vajont Landslide

The Vajont valley is located in the western part of Friuli Venezia Giulia region, in Italy. The topographic boundaries of the Vajont valley are the S. Osvaldo pass on the east, the Tóc mount on the south, the SADE dam on the west and the mount Borga on the north. The valley is oriented east-west and was formed as the result of the erosion of an ancient glacier. The two main waterways are the Vajont stream which gives the name to the valley and its major tributary, the stream Mesazzo (see figure 7).

Figure 5: Aerial view of the Vajont and Piave valleis.

At about 10 pm of 9^{th} October 1963, approximately 270 millions cubic meters of material slid from the mount Toc into the dam reservoir, generating a huge wave that overtopped the dam destroying the town of Longarone in the Piave valley, downstream the dam. The landslide

produced a wave that has been estimated to have reached a height of about 105 meters above the the dam crest. Due to the irregular terrain topography, the wave did not reach the same elevation around the reservoir, as could be determined observing the contour of destroyed vegetation. In the Piave valley, the effects were much more destructive: the city of Longarone was almost completely destroyed, only a portion of the city at the north was not affected; the same happened for the surrounding villages of Villanova and Fa. Over 2000 people were killed and this is considered to have been one of the most disastrous landslides occurred in the XX century.

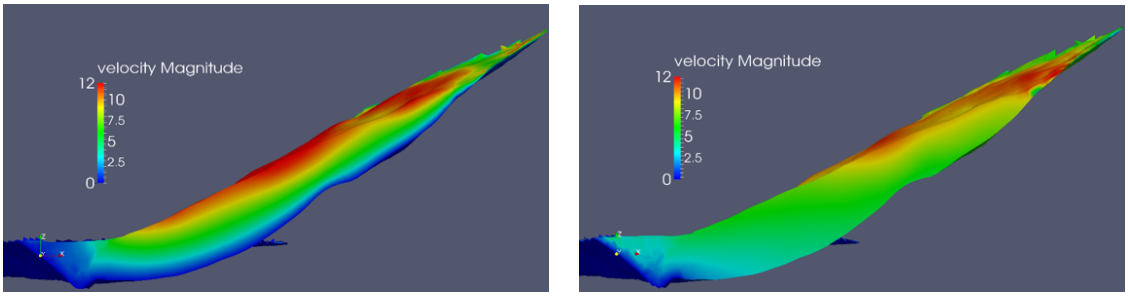

(a) $h_{slip} = 5m$ (b) $h_{slip} = 500m$

Figure 6: Vajont Slide. Effect of the slip boundary conditions.

The previously described numerical technique is here used for the simulation of the complete sequence of events: landslide runout, interaction with the water reservoir and generation of the overtopping wave. Other numerical simulations of this tragedy have been reported in [14, 15]. Table 2 summarizes the parameters used in the simulation [14].

	terrain	water
ρ	$2.4\ 10^3\ Kg/m^3$	$10^3\ Kg/m^3$
ϕ	$26°$	-
ϕ_{basal}	$5°$	-
μ_0	$0.1\ Pa\ s$	$0.001\ Pa\ s$
h_{slip}	$500\ m$	-

Table 2: Vajont Landslide. Material parameters.

For the numerical analysis, a finite element mesh of 78137 nodes has been used with a fixed time step of 10^{-2} seconds. The effect of the slip boundary conditions can be appreciated in Figure 6, where two velocity profiles are plotted for varying slip length. As expected, it can be observed that a larger value of the slip length leads to a more homogeneous velocity profile, which is consistent with the almost rigid motion of the sliding mass observed in reality.

Figure 8 shows snapshots of the numerical simulation at different time instants while figure 7 shows a comparison between numerical results and post-event surveys of the maximum elevation reached by the wave on the right bank. A satisfactory agreement can be noted, with discrepancies mainly due to the coarse adopted discretization. The estimated overtopping height is of 100 meters, which closely matches the observed one.

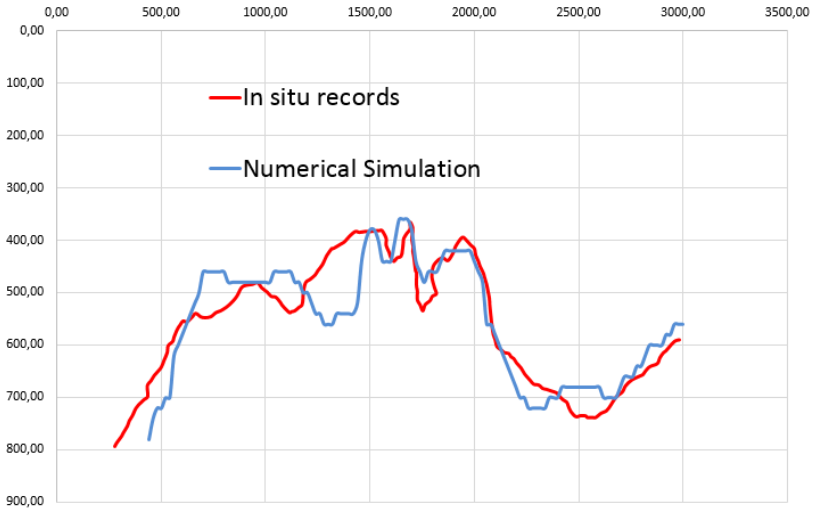

Figure 7: Vajont Slide. Maximum height of the wave reached in the right bank.

8 CONCLUSIONS

In the present work, a Lagrangian finite element method has been presented for the numerical simulation of landslide-water interaction. The landslide has been modeled as a viscoplastic non-Newtonian frictional fluid while water as a standard Newtonian fluid. Slip boundary conditions have been introduced between the landslide and the slope to better represent the real behavior of the basal interface. To validate the proposed approach, the proposed approach has been applied to two real landslides. The second example in particular concerned the simulation of a complex event, consisting of a landslide impinging in a water reservoir and generating a wave overtopping an existing concrete dam. Good accuracy has been obtained in the simulations.

REFERENCES

[1] Quecedo, M., Pastor, M. and Herreros, M.I. Numerical modelling of impulse wave generated by fast landslides. *International Journal for Numerical Methods in Engineering* (2004) **59**:1633–1656.

[2] Cremonesi, M., Frangi, A. and Perego, U. A Lagrangian finite element approach for the simulation of water-waves induced by landslides. *Computers and Structures* (2011) **89**:1086–1093.

[3] Cremonesi, Frangi, A. and Perego, U. A Lagrangian finite element approach for the analysis of fluidstructure interaction problems. *International Journal for Numerical Methods in Engineering* (2010) **84**:610–630.

[4] Cremonesi, M., Ferrara, L., Frangi, A. and Perego, U. Simulation of the flow of fresh cement suspensions by a Lagrangian finite element approach. *Journal of Non-Newtonian Fluid Mechanics* (2010) **165**:1555–1563.

[5] Oñate, E., Idelsohn, S.R., del Pin, F. and Aubry, R. The Particle Finite Element Method. An Overview. *International Journal Computational Method* (2004) **1**:267–307.

[6] Idelsohn, S.R., Oñate, E. and del Pin, F., The Particle Finite Element Method: A Powerful tool to Solve Incompresible Flows with Free-Surfaces and Breaking Waves. *International Journal for Numerical Methods in Engineering* (2004) **61**:964–989.

[7] Idelsohn, S.R., Oñate, E., del Pin, F. and Calvo, N., Fluid Structure Interaction Using the Particle Finite Element Method. *Computer Methods in Applied Mechanics and Engineering* (2006) **195**:2100–2123.

[8] Donea, J. and Huerta, A., Finite Element Methods for Flow Problems. *Wiley* (2005).

[9] Papanastasiou, T.C., Flows of materials with yield *Journal of Rheology* (1987) **31**:385–404.

[10] Cremonesi, M., Ferri, F., and Perego, U. A basal slip model for Lagrangian finite element simulations of 3D landslides. *submitted for publication*.

[11] Dawson, R F, Morgenstern, N R and Stokes, W Liquefaction flowslides in Rocky Mountain coal mine waste dumps. *Canadian Geotechnical Journal*. (1998) **35**:328–343.

[12] Pastor, M. and Blanc, T. and Haddad, B. and Petrone, S. and Sanchez Morles, M. and Drempetic, V. and Issler, D. and Crosta, G. B. and Cascini, L. and Sorbino, G. and Cuomo, S. Application of a SPH depth-integrated model to landslide run-out analysis. *Landslides*. (2014) **11**:793–812.

[13] Herrores, M. I. and Fernández Merodo, J. a. and Quecedo, M. and Mira, P. and Pastor, M. and GonzÁlez, E. Modelling tailings dams and mine waste dumps failures. *Géotechnique* (2002) **52**:579–591.

[14] Crosta, G.B., Imposimato, S. and Roddeman, D., Landslide Spreading, Impulse Water Waves and Modelling of the Vajont Rockslide. *Rock Mechanics and Rock Engineering* (2015):1-24.

[15] Vacondio, R., Mignosa,P. and Pagani, S. 3D SPH numerical simulation of the wave generated by the Vajont rockslide. *Advances in Water Resources* (2013) **59**:146 - 156.